Catena 267 (2026) 110003

Contents lists available at ScienceDirect

Catena

journal homepage: www.elsevier.com/locate/catena

Century-long afforestation induces microbial metabolic nitrogen limitation with soil fungal community dominating the process

Jiangbing Xu [a,*], Yuhao Wu [a], Song Jin [b], Haiquan Guo [b,c], Lei Liu [a], Jing Meng [d], Guoyi Zhou [a,*]

[a] Institute of Ecology, School of Ecology and Applied Meteorology, Nanjing University of Information Science and Technology, Nanjing 210044, China
[b] Hebei Geological Survey Institute, Shijiazhuang 050200, China
[c] Geological Exploration Technology Center of Hebei Bureau of Geology and Mineral Resources Exploration, Shijiazhuang 050081, China
[d] National Nature Reserve Management Center of Liujiang Basin Geological Relics, Qinhuangdao 066000, China

ARTICLE INFO

Dataset link: PRJNA1208408 (Original data)

Keywords:
Afforestation
Soil ecoenzymatic stoichiometry
Metabolic N limitation
Fungi

ABSTRACT

Afforestation is a vital strategy for restoring ecological balance, mitigating climate change, and conserving biodiversity. Soil microbial metabolic limitations, critical for forest ecosystem functions, are strongly influenced by stand age, yet their responses to stand age and their relationship with soil microbial community remain unclear. In this study, we collected soil samples from a temperate forest located in Northeast China, representing stand ages of 0, 10, 40, 80, and 160 years (denoted as y0, y10, y40, y80, and y160, respectively). Soil enzyme activities related to C-, N-, and P-acquisition were measured using a fluorescence method, with subsequent ecoenzymatic stoichiometry analysis to assess microbial metabolic limitation. The soil bacterial and fungal communities were characterized by high-throughput sequencing. Results showed that while long-term afforestation generally increased the enzyme activities, microbial metabolism remained primarily N limited— a limitation that intensified with stand age. The attributes of soil fungal community (i.e., alpha-diversity, composition, and the function groups) were more susceptible to the soil enzyme activities and metabolic N limitation under afforestation, rather than those of the bacterial community. The enriched fungal taxa comprised both ectomycorrhizal and saprotrophic fungi, which showed opposing responses to metabolic N limitation (positive and negative, respectively). Taken together, our findings underscore the close relationship between soil fungal community and the enzymatic properties over centennial timescales, advancing our understanding of microbial adaptation to long-term afforestation.

1. Introduction

Afforestation is recognized as a crucial strategy for preventing wind erosion, maintaining biodiversity, conserving water resources, increasing carbon (C) storage, and regulating global climate change (Bonan, 2008). Assessing its effectiveness necessitates a mechanistic understanding of the underlying ecological processes. During afforestation, litterfall inputs and root dynamics reshape the allocation of nutrient elements between above- and below-ground systems (Zheng et al., 2024). This shift subsequently modifies soil microbial-driven nutrient cycling and, in turn, affects forest productivity. Thus, understanding how afforestation influences soil microorganisms and nutrient dynamics is essential for evaluating the overall success of afforestation.

Soil microorganisms acquire C, nitrogen (N), and phosphorus (P) by secreting extracellular enzymes that catalyze the depolymerization of organic matter. This makes soil enzymes reliable indicators of microbial activity and soil ecological functions (Yadav et al., 2021). Under conditions of nutrient limitation, microorganisms upregulate targeted extracellular enzymes to break down complex organic polymers and meet their nutrient demands. Accordingly, ecoenzymatic stoichiometry, i.e., the ratios of C-, N- and P-acquiring enzymes, reflects the match between microbial nutrient demands and environmental supply, serving as a robust proxy for microbial metabolic efficiency and nutrient limitations (Liu et al., 2024a). In recent decades, although an extensive body of research has evaluated the soil microbial metabolic limitations during afforestation, the reported patterns vary profoundly. For example, some studies indicate an aggravated metabolic N limitation with stand age (Du et al., 2024; Yan et al., 2022), while others find that afforestation alleviates such limitation (Liu et al., 2024a). Zhao et al. (2025) observe the strongest C and N limitations in middle-aged stands, with

* Corresponding authors at: No. 219, Ningliu Road, Nanjing University of Information Science and Technology, Nanjing 210044, China.
E-mail addresses: jbxu@nuist.edu.cn (J. Xu), gyzhou@nuist.edu.cn (G. Zhou).

https://doi.org/10.1016/j.catena.2026.110003
Received 29 August 2025; Received in revised form 1 February 2026; Accepted 7 March 2026
0341-8162/© 2026 Elsevier B.V. All rights are reserved, including those for text and data mining, AI training, and similar technologies.

comparatively weaker limitations in mature stands. This pattern aligns with the known negative relationship between plant productivity and microbial C limitation (Deng et al., 2019). Cui et al. (2020) document a shift from weak P limitation in the early-stage forest (35 years) to strong P limitation in the older forest (130 years). Taken together, these contrasting findings suggest that the response of soil microbial metabolic limitation to afforestation remains unclear.

Soil microorganisms are primary producers of extracellular enzymes and fundamental drivers of soil nutrient cycling. In forest ecosystems, although microbial community responses to afforestation have been widely studied, the consequences remain controversial. Some studies report more pronounced shifts in bacterial community than in fungal community along a stand-age chronosequence (Liang et al., 2021), while others report the opposite pattern (Wan et al., 2021; Zhao et al., 2025). Still other study finds no significant effect of stand age on fungal guilds (Odriozola et al., 2020). These discrepancies may be linked to divergent changes in soil environmental factors across different stand ages, such as microclimate, litter quality, and resource availability (Wan et al., 2021). Notably, with increasing stand age, the accumulation of recalcitrant soil compounds (e.g., lignin) substantially alters microbial nutrient-acquisition strategies, thereby favoring certain microbial lineages. Fungi, compared with bacteria, may be favored and impacted due to their higher C-use efficiency than bacteria (Rosinger et al., 2019; Veres et al., 2015). This implies that shifts in fungal community structure could become more obvious over long-term afforestation. Given the uncertainty of soil microbial metabolic limitation during afforestation, the specific microbial groups associated with these variations remain unclear and warrant further investigation.

In this study, we selected the Saihanba Mechanized Forest Farm in China's northeastern Mollisols region as our study site due to its century-long history of afforestation, which provided an ideal setting for studying the long-term afforestation effects on soil microbial properties. We established a stand-age chronosequence (0, 10, 40, 80, and 160 years) within the dominant forest species and collected soil samples accordingly. Soil enzyme activities were quantified using the fluorometric assays, and the microbial community was characterized by high-throughput sequencing of the bacterial 16S rRNA and fungal ITS regions. Our aim was to reveal the patterns of microbial metabolic limitation and the associated community shifts across the chronosequence. Three hypotheses were proposed: 1) soil nutrient contents increased with stand age due to the successive inputs of organic materials; 2) soil microorganisms experienced persistent N limitation across the chronosequence, which became more severe in older stands; 3) soil fungal community might play a more significant role than the bacterial community in response to the metabolic N limitation, as fungi are more efficient in acquiring N from recalcitrant organic compounds.

2. Materials and methods

2.1. Experimental site and soil sampling

The study was conducted in the Saihanba Mechanized Forest Farm, Hebei, China (116°51′-117°39′E, 42°02′-42°40′N), on the southern edge of the Inner Mongolia Plateau, bordering the Hunshandake Sandy Land. The region features aeolian, meadow, and boggy soils, characterized by a continental monsoon climate with an average annual temperature of −1.4 °C and precipitation of 450.1 mm, and a frost-free season of 67 days. The upper boundary of the landform is between the plateau and the mountains, and it belongs to the forest-grassland transition zone. The soil is predominantly sandy and defined as inceptisols in the soil taxonomy system of the United States, and it is categorized as a gray-forest soil in China's soil classification system (Yao et al., 2020). This region has a large area of afforestation with a history spanning over a century. Mongolian pine (*Pinus sylvestris* var. *mongolica*) is the dominant tree species here due to its high tolerance to cold, drought, and soil infertility (Sukhbaatar et al., 2019).

The present study used the "space-for-time" approach to explore the changes of soil enzymatic and microbial characteristics along the afforestation chronosequence (Liang et al., 2021). Soil samples were collected from Mongolian pine stands of five different ages: 0, 10, 40, 80, and 160 years (denoted as y0, y10, y40, y80, and y160, respectively; ages were confirmed by local forestry records). The y0 site was converted from barren land to a Mongolian pine (*Pinus sylvestris* var. *mongolica*) plantation within less than a year. All sites were located within a 3-km radius to ensure consistent climate, soil conditions, and initial planting density across all sites (Fig. 1). No post-afforestation fertilization or irrigation was implemented. Soil samples was collected in May 2023. At each site, we established five independent sampling locations, spaced at least 20 m apart to ensure spatial independence. After removing the ground litter layer at each location, we collected five soil cores (0–20 cm depth) using a 5-cm diameter drilling sampler from a 2 m × 2 m quadrat. The five cores from the same quadrat were homogenized to form one composite sample, representing one biological replicate. This sampling design resulted in five independent biological replicates (composite samples) per stand age, yielding a total of 25 samples (5 ages × 5 replicates). The soil samples were immediately stored at 4 °C in a portable fridge and transported to the laboratory within 24 h. In laboratory, all samples were sieved (2 mm) to remove roots and debris. Soil enzyme activities were analyzed immediately. The remaining samples were separated into two portions: one portion was air-dried, ground, and re-sieved (0.149 mm) for chemical analysis, while the other was stored at −40 °C for molecular analysis.

2.2. Measurement of soil chemical properties

Soil water content (SW, %) was determined gravimetrically by drying the samples at 105 °C. Soil pH was measured using a pH meter with a 1:2.5 soil-to-water suspension (*w/v*). Soil electrical conductivity (EC, mS/cm) was measured using a conductivity meter (DDS-307, LeiCi, Shanghai, China) on a 1:5 soil to water extraction (w/v) of each sample. Soil organic C (SOC, g/kg) and total N (TN, g/kg) were determined using a Vario El cube elemental analyzer (Elementar, Germany). Ammonium N (NH_4^+-N, mg/kg) and nitrate N (NO_3^--N, mg/kg) were extracted with 0.5 mol/L KCl, and measured with a continuous-flow injection analyzer (Skalar Analytical SAN $^{++}$ Instruments, Breda, Netherlands). Total P (TP, g/kg) was assayed using the molybdenum antimony colorimetric method after HF-$HClO_4$ digestion, and Olsen-P (AvailP, mg/kg) was determined using the same method but after 0.5 mol/L $NaHCO_3$ extraction at pH 8.5.

2.3. Determination of soil enzyme activities and calculation of ecoenzymatic stoichiometry

The extracellular enzyme activities were measured using highly fluorescent compounds 7-amino-4-methylcoumarin and 4-methylumbelliferone as substrates (Saiya-Cork et al., 2002; Sinsabaugh et al., 2008). The tested enzymes included C-acquisition enzymes (β-1,4-glucosidase, BG), N-acquisition enzymes (β-*N*-acetylglucosaminidase, NAG; and L-leucine aminopeptidase, LAP), and the P-acquisition enzyme (acid phosphatase, AP). BG catalyzes the hydrolysis of cellobiose and cellodextrins into glucose (Veres et al., 2015), the last step of cellulose degradation. NAG degrades chitin—a major component of fungal cell walls and arthropod exoskeletons—yielding *N*-acetylglucosamine, whereas LAP hydrolyzes peptide bonds to release free amino acids (Daunoras et al., 2024). AP is responsible for mineralization of organic matter to release phosphate ions ($H_2PO_4^-$ and HPO_4^{2-}) in soil (Criquet and Braud, 2008). The specific enzyme substrates used for each enzyme are shown in Table S1. From the fluorescent values and standard calibration curves, the activity of each enzyme was calculated and expressed as nanomoles per gram of dry soil per hour (nmol/g /h).

Two ecoenzymatic stoichiometry models were applied to evaluate the microbial metabolic limitations, i.e. the vector analysis and the

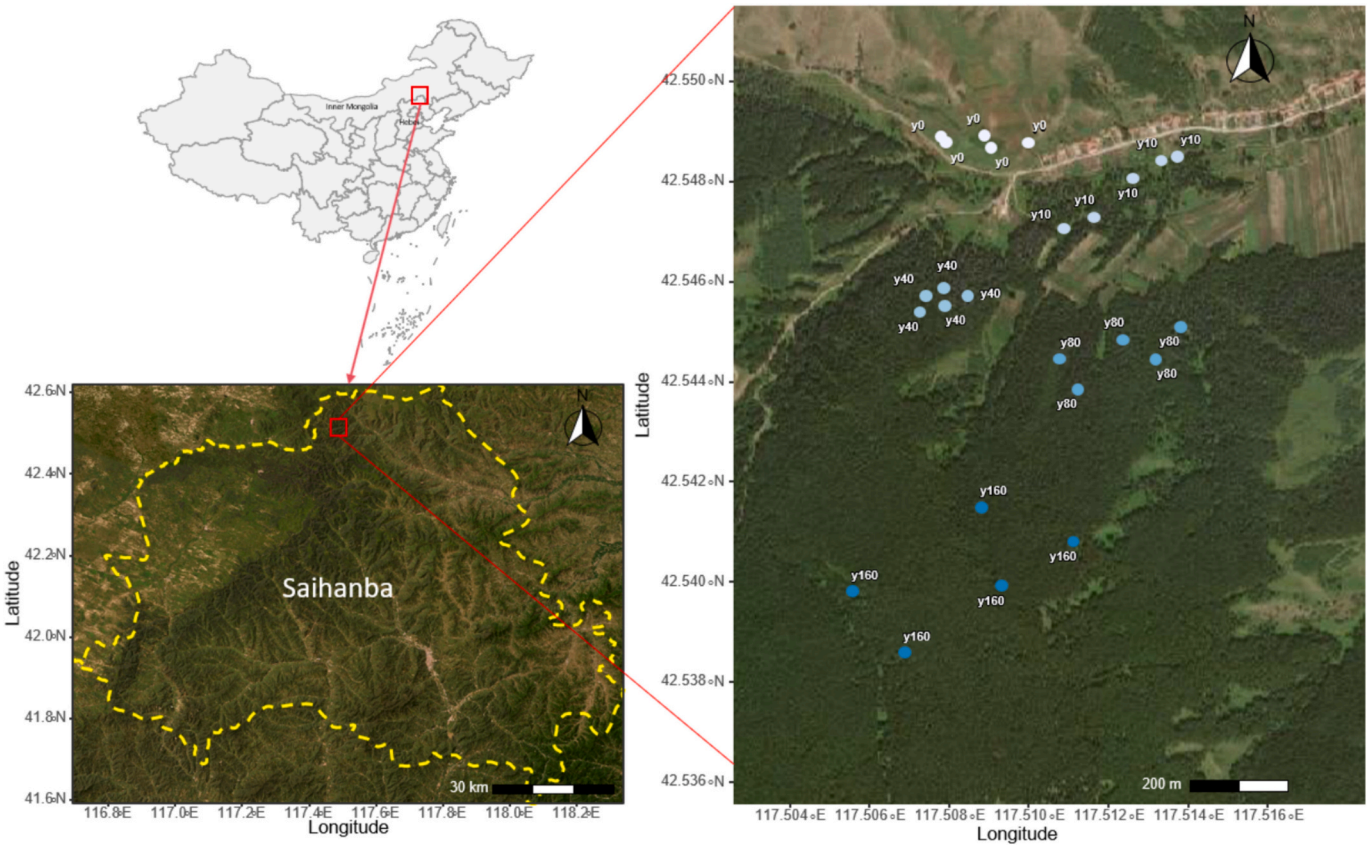

Fig. 1. Location of the study area and the sampling site. The labels y0, y10, y40, y80, and y160 represent afforestation stands aged 0, 10, 40, 80, and 160 years, respectively.

threshold model.

The vector analysis was conducted to demonstrate the microbial resource limitation (Moorhead et al., 2016).

$$\text{Vector length (L, unitless)} = \sqrt{x^2 + y^2} \quad (1)$$

$$\text{Vector angle } (A^o) = \text{Degrees (ATAN2(x, y))} \quad (2)$$

where x is the relative activity of C-acquisition enzyme to P-acquisition enzyme calculated by BG/(BG + AP); y is the relative activity of C-acquisition enzyme to N-acquisition enzyme calculated by the untransformed proportional activities as BG/(BG + LAP+NAG). Vector length represents relative C versus nutrient (N or P) limitation, with a relatively longer value indicating greater C limitation. Generally, vector angle>45° is considered to be relatively more limited by P than N, with the opposite interpretation for the lower angle (Sinsabaugh and Follstad Shah, 2012). Nevertheless, a recent study finds that the equilibrium point where P becomes more limiting than N varies with the substrate quantity and ecosystem type (Cui et al., 2024). Specifically, the authors proposed that a vector angle of 55° represents a more appropriate equilibrium point in cellulose-dominated ecosystems such as forest—a criterion we adopted in this study.

The threshold model was conducted following the procedure described by Cui et al. (2021, 2023).

$$\text{Metabolic N limitation} = \ln\left(1.5\frac{n0}{EEA_{C:N}}\right) \quad (3)$$

$$\text{Metabolic P limitation} = \ln\left(1.5\frac{p0}{EEA_{C:P}}\right) \quad (4)$$

$$\text{Metabolic C limitation} = \ln\left(\frac{EEA_{C:N} \times EEA_{C:P}}{2.25(n0 \times p0)}\right) \quad (5)$$

where *n0* and *p0* parameters are determined by regression relationships among C-, N- and P-acquisition enzyme activities, i.e., $n0 = e^{\text{intercept}}$ in the regression for ln(BG) vs. ln(NAG+LAP) and $p0 = e^{\text{intercept}}$ in the regression for ln(BG) vs. ln(AP). $EEA_{C:N}$ and $EEA_{C:P}$ are calculated by BG/(LAP+ NAG) and BG/AP, respectively. Values of metabolic N limitation, metabolic P limitation, and metabolic C limitation greater than 0 indicate N, P, and C limitation, respectively, with greater values denoting stronger limitation.

2.4. DNA extraction, high-throughput sequencing, and data processing

Soil genomic DNA was extracted from 0.5 g fresh soil samples, using a DNA extraction kit (MP Biomedicals, Santa Ana, CA, USA). The purity and concentration of the DNA were analyzed using a nucleic acid protein quantizer, NanoDrop One (Thermo Scientific, Waltham, MA, USA). DNA integrity was evaluated using 2% agarose gel electrophoresis (Applied Biosystems, Waltham, MA, USA). Each DNA sample was measured and placed in a centrifuge tube before being diluted with sterile water to 1 ng/μL. The diluted genomic DNA was used in PCR along with high-fidelity DNA polymerase (5 U/L) and specific primers with barcodes. The bacterial 16S rRNA gene sections V4-V5 were amplified using the primers 515F (5'-GTGCCAGCMGCC GCGG-3′) and 907R (5'-CCGTCAATTCMTTTRAGTTT-3′). The internal transcribed spacer region of fungi was amplified using the ITS1F (5′-GGAAG AAAAGTCGTAA-CAAGG-3′) and ITS2R (5'-GCT GCGTTCTTCATCGATGC-3′) primers (Douglas et al., 2020; Wang et al., 2024). Amplicons of bacterial 16S and fungal ITS genes were subjected to metagenomic sequencing using Illumina MiSeq platform (Illumina, CA, USA) at the Majorbio Bio-Pharm Technology Co., Ltd. (Shanghai, China) according to standard manufacturer protocols.

Raw sequence data were demultiplexed and quality-filtered using the

DADA2 algorithm implemented in QIIME 2. The generated amplicon sequence variants (ASVs) were subsequently aligned against the reference database Silva v138 to obtain taxonomical information of each ASV based on 100% sequence similarity. The sequences were then rarefied for downstream analysis. The raw sequencing reads were deposited into the National Center for Biotechnology Information (NCBI) Sequence Read Archive (SRA) database under the accession number PRJNA1208408.

2.5. Data analysis

All subsequent bioinformatics analyses, data visualization, and statistical computations were performed using R v4.3.3. A one-way analysis of variance (ANOVA) incorporating Tukey's post hoc test was conducted to determine variations in soil chemical and enzymatic properties among samples with different stand ages. The Shapiro-Wilk test was used to determine the normality of the data before statistical analysis, and logarithmic transformations were used if necessary. A significance level of $p < 0.05$ was adopted throughout, unless otherwise stated. Niche width, calculated using Levins' index, was performed with the spaa package (V0.2.5) based on microbial genus-level abundance. Principal coordinates analysis (PCoA) was applied to evaluate the structural difference within the microbial community based on the Bray-Curtis distances. Pairwise PERMANOVA was performed to discern the differences in the microbial community structure using the pairwiseAdonis package. Bonferroni *P*-value correction was applied as the default method for multiple comparisons. Linear discriminant analysis (LDA) Effect Size (LEfSe) implemented with the microeco package (Liu et al., 2021), was used to identify the most differentially abundant microbial taxa across stand ages. An LDA score threshold (log10) of 2 was used to distinguish characteristics, and the Kruskal-Wallis sum-rank test was used to identify significant differences ($p < 0.05$) among treatments. FAPROTAX and FUNGuild database to predict bacterial and fungal functional groups (Jiang et al., 2021).

Relationships among soil chemical, microbial, and enzymatic properties were assessed using random forest analysis and Spearman correlation analysis. Subsequently, partial least squares-path modeling analysis (PLS-PM) was conducted with the plspm package to explore their direct and indirect pathways. The analysis was based on an initial hypothesized conceptual model that included all reasonable paths linking environmental factors, microbial community properties, and ecoenzymatic stoichiometry. Non-significant pathways were then sequentially eliminated until all remaining paths were significant ($p < 0.05$). Variables with loadings <0.7 were removed, and the goodness-of-fit index (GOF) and R^2 were used to estimate model performance.

3. Results

3.1. Soil chemical properties

Across the chronosequence, the soil chemical properties, including SW, EC, SOC, and TN, showed similar increasing trends (Fig. 2), with peak values observed in y160, significantly higher than those in the other periods ($p < 0.05$). Soil pH decreased significantly in the early period (<40 years), followed by an increase after 80 years, approaching the initial pH value. Significant increases of NH_4-N and TP occurred in

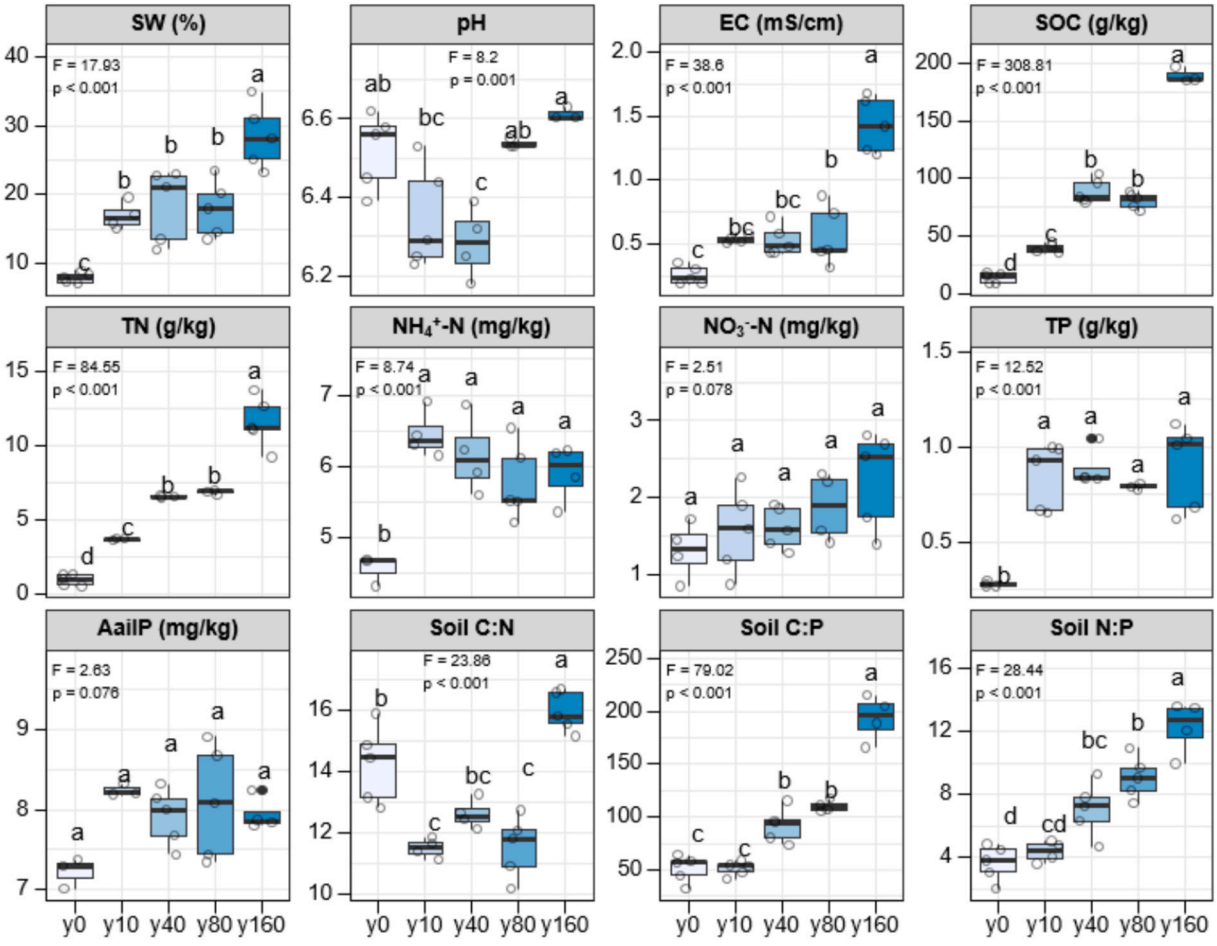

Fig. 2. Soil chemical properties across the afforestation chronosequence. The labels y0, y10, y40, y80, and y160 represent afforestation stands aged 0, 10, 40, 80, and 160 years, respectively. SW, soil water content; EC, electrical conductivity; SOC, soil organic carbon; TN, total nitrogen; TP, total phosphorus; AvailP, available P.

y10 ($p < 0.05$), and then remained steady thereafter. NO_3^-N showed an increasing but non-significant trend as the stand age increased ($p > 0.05$). The ratios of soil C:P and N:P displayed different patterns; soil C:P and N:P ratios increased across the chronosequence, while soil C: N followed an open unimodal pattern with a significantly lower value in y10.

3.2. Soil enzyme activities and ecoenzymatic stoichiometry

The activities of C-acquisition (BG), N-acquisition (NAG and LAP), and P-acquisition enzymes (AP) exhibited similar trends across the chronosequence, i.e. the gradual increase in the first 40 years, followed by a sudden decrease in y80, and then a significant increase in y160 (Fig. 3A). The vector analysis showed that the vector length ranged from 0.64 to 0.78, but these values did not significantly differ across the chronosequence ($p > 0.05$). The vector angle increased in the initial 10 years before declining linearly from y10 (50.8°) to y160 (41.05°) (Fig. 3B, $p < 0.05$). Consistently, the threshold model revealed that the values of metabolic N limitation were all above zero. After an initial significant decrease from y0 to y10 ($p < 0.05$), the metabolic N limitation demonstrated a subsequent linear increase from y10 to y160 (Fig. 3C). The values of metabolic C limitation were all below zero and did not significantly differ ($p > 0.05$), indicating no C limitation. The values of metabolic P limitation increased significantly during the first 10 years ($p < 0.05$), but remained relatively stable thereafter ($p > 0.05$). Given that all vector angles remained below 55° and the magnitude of metabolic P limitation was consistently low (only slightly above zero), we concluded that afforestation exerted only a weak long-term effect on metabolic P limitation.

3.3. Soil microbial community composition

In all samples, the dominant bacterial phyla were Proteobacteria (22.80–39.35%), Actinobacteria (14.97–30.15%), Acidobacteria (13.08–25.05%), and Chloroflexi (2.5–7.45%); and the dominant fungal phyla were Basidiomycota (9.71–76.68%), Ascomycota (10.98–64.66%), Monoblepharomycota (0.93–25.8%), and Rozellomycota (0.04–10.83%) (Fig. S1). With increasing stand age, the relative abundance of Ascomycota increased while that of Basidiomycota declined. A total of 56 bacterial genera exhibited significant differences across the afforestation chronosequence (LDA > 2, $p < 0.05$, Fig. S2). Clear successional shifts were observed in both communities. Specifically, bacterial community composition shifted from being enriched in Sphingobacteriales, Micrococcales, Sphingomonadales, and Pyrinomonadales in y0, to *Microlunatus* and Acidobacteriales in y10, and ultimately to *Methyloligellaceae* and *Clostridium* in y160 (Fig. S2A). The fungal community transitioned from an early enrichment of *Geminibasidium* in y0, to Lipomycetaceae in y40, and then to Myxotrichaceae, *Cladophialophora,* Cortinariaceae, Sebacinales, *Oidiodendron,* and *Russula* in y80, and finally to Coniochaetaceae and *Tausonia* in y160 (Fig. S2B).

3.4. Alpha- and beta-diversity of soil microbial community

Afforestation across the chronosequence altered the alpha-diversity and beta-diversity of soil bacterial and fungal communities to varying degrees (Fig. S3). Generally, the alpha-diversity indices of the soil bacterial community remained relatively stable across the chronosequence. In contrast, the Chao1 and Shannon indices for the fungal community over time steadily increased ($p < 0.05$), indicating their sensitive responses to afforestation. As stand age increased, the fungal niche width showed a significant upward trend ($p < 0.05$), whereas the bacterial niche width did not significantly change (Fig. S4). PCoA results indicated that both bacterial and fungal community structures underwent significant changes across the chronosequence ($p < 0.01$). Pairwise adonis analysis further revealed that both the bacterial and fungal communities significantly changed with different stand ages during the afforestation (Table S2).

3.5. Soil microbial putative functions

The predicted microbial functions that differed significantly across the chronosequence are illustrated in Fig. S5 and Fig. 4, respectively, based on FAPROTAX (bacteria) and FUNGuild (fungi). In the bacterial community, only cellulolysis that links to organic compound decomposition showed a significant change, increasing initially (<40 years, $p < 0.05$) and then decreased in later period (>80 years, $p < 0.05$) (Fig. S5). For fungal community, the relative abundance of saprotroph

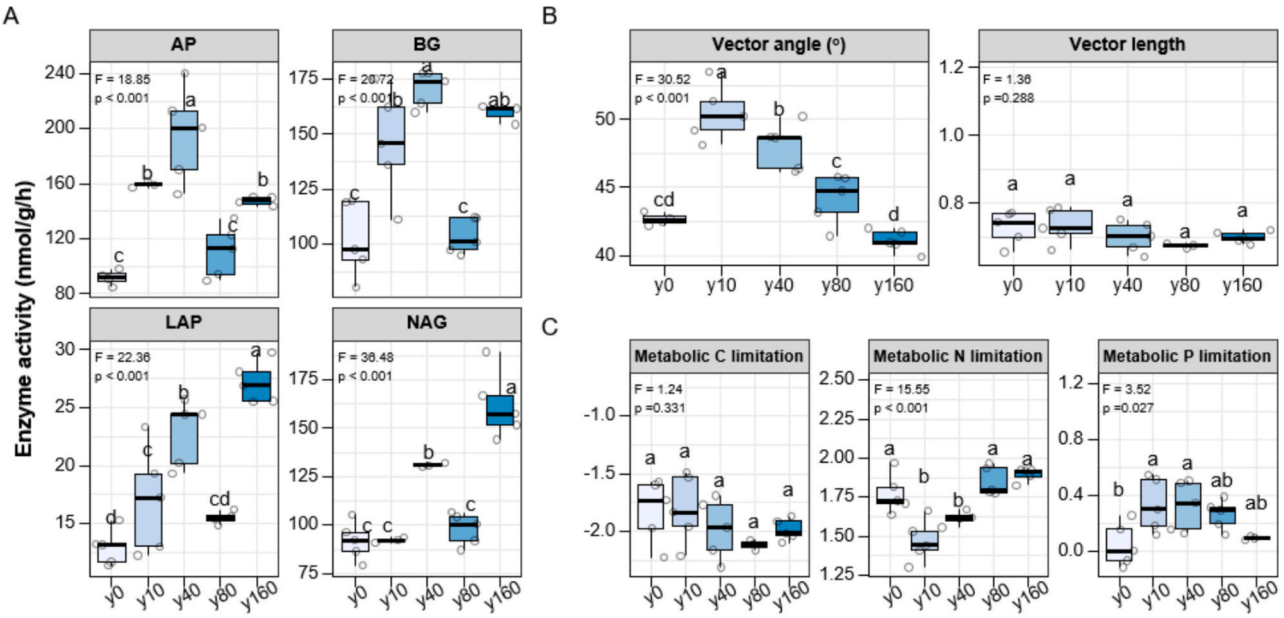

Fig. 3. Soil enzyme activities (A), vector analysis (B), and nutrient threshold model (C) across the afforestation chronosequence. The labels y0, y10, y40, y80, and y160 represent afforestation stands aged 0, 10, 40, 80, and 160 years, respectively. AP, acidic phosphatase; BG, β-1,4- glucosidase; BX, β-xylosidase; CBH, β-D-cellobiohydrolase; LAP, leucine aminopeptidase; NAG, β-*N*-acetylglucosaminidase.

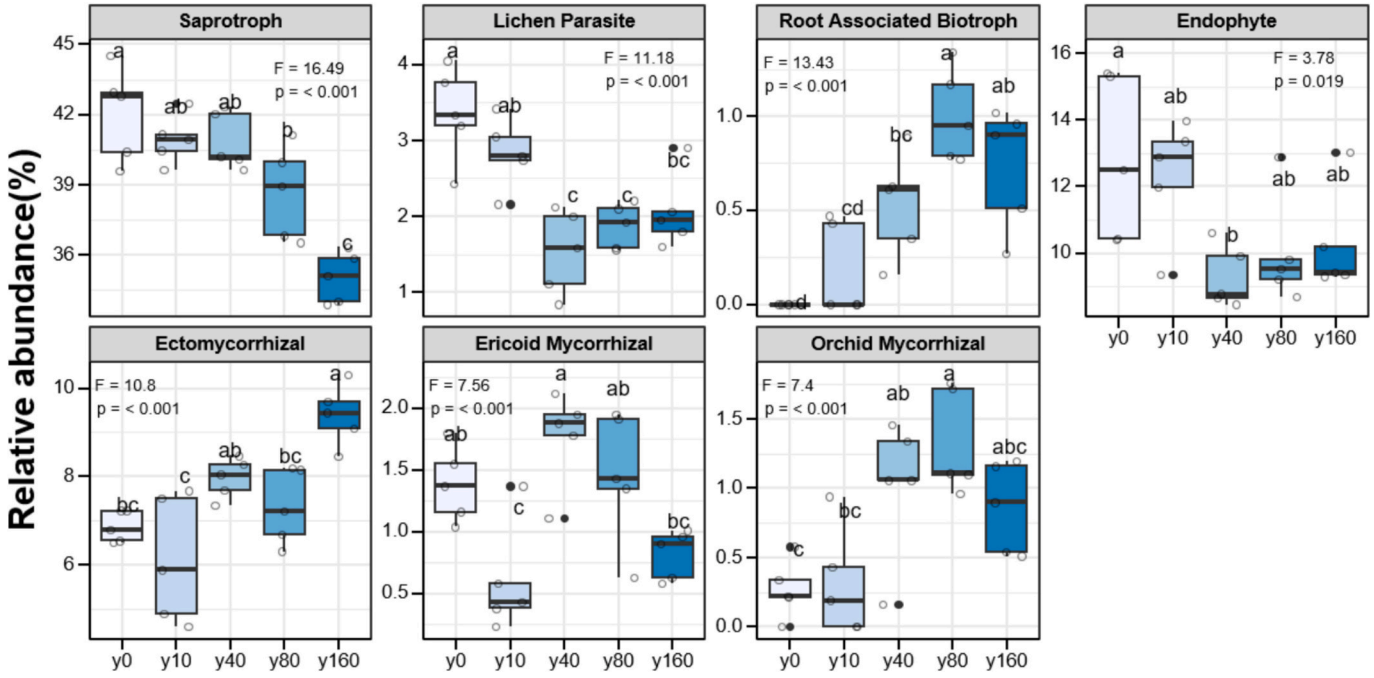

Fig. 4. Differences in fungal putative functions obtained by FUNguild. Different letters within each function indicate statistically significant differences in soils of different stand ages ($p < 0.05$). The labels y0, y10, y40, y80, and y160 represent afforestation stands aged 0, 10, 40, 80, and 160 years, respectively.

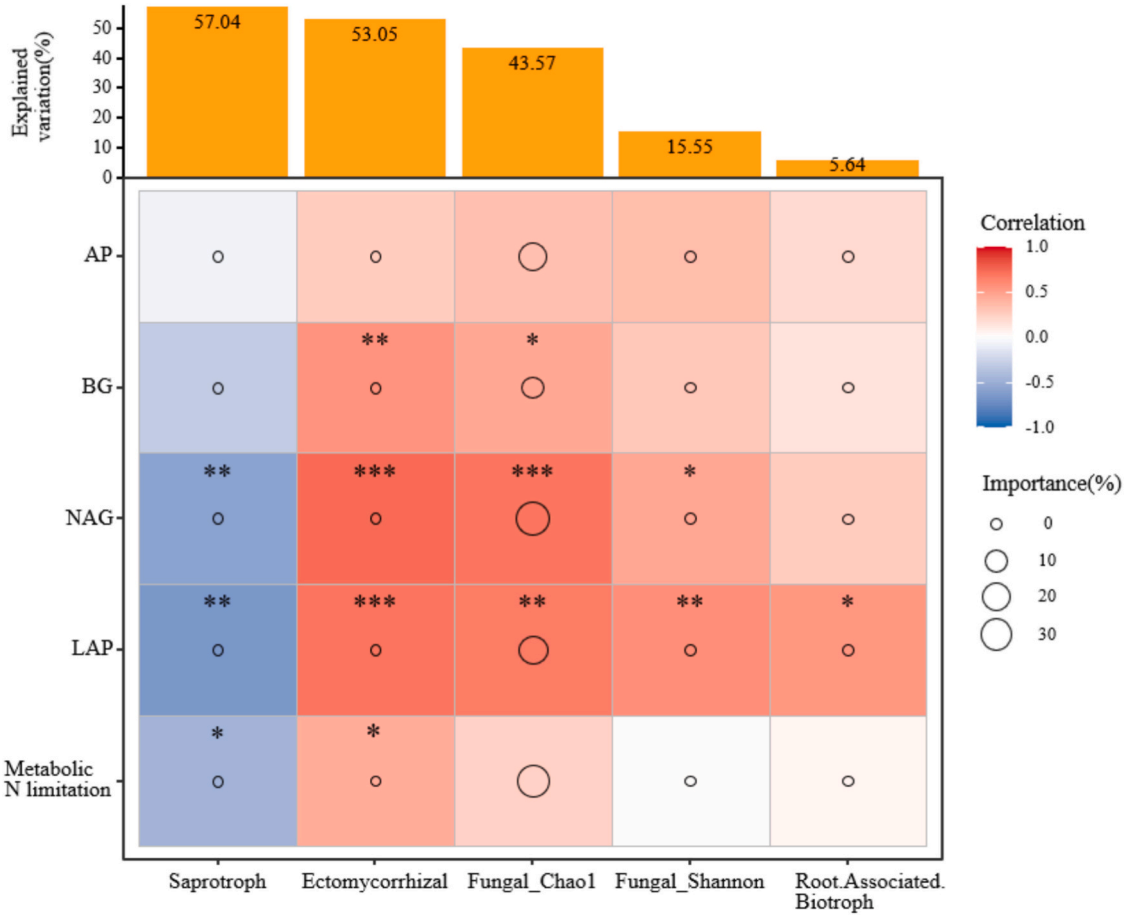

Fig. 5. Relationships between soil fungal community and soil enzymatic properties. The heatmap plots illustrate their Spearman correlations, and the circles over diamonds symbolize the importance of soil enzymatic properties on the fungal community properties. The total explained variations of those factors are summed and displayed over the heatmap using the bar chart. The asterisk indicates significant correlations. *, $p < 0.05$, **, $p < 0.01$, ***, $p < 0.001$.

showed a deceasing trend across the chronosequence, with a significant lower value in y160 than in y80 and y0 ($p < 0.05$, Fig. 4). In contrast, ectomycorrhizal fungi increased with stand age, displaying significantly lower abundance in y160 than in y10 and y0 ($p < 0.05$). Other fungal functions such lichen parasite and endophyte decreased significantly in the early period (<40 years, $p < 0.05$) but showed no significant differences thereafter. The root-associated biotroph and orchid mycorrhiza displayed increasing trends up to 80 years, with significantly higher proportions in y80 than in y0 ($p < 0.05$, Fig. 4). No significant variation was observed thereafter.

3.6. Relationships among soil chemical, microbial, and enzymatic properties

We then analyzed the influences of soil enzymatic properties on soil microbial community. Based on the random forest analysis, we found that only fungal putative functions and alpha diversity were profoundly influenced, rather than the bacterial (The explained variations for the bacterial community were below 5% and were therefore not presented in Fig. 5). Metabolic N limitation and enzyme activities together accounted for 57.04%, 53.05%, 43.57%, and 15.55% of the total variance in Saprotrophic fungi, ectomycorrhizal fungi, fungal Chao1 index, and fungal Shannon index, respectively (Fig. 5). Spearman correlation analysis revealed the distinct relationships between soil fungal community attributes and enzymatic properties (Fig. 5). Specifically, the relative abundance of saprotrophs was negatively correlated with N-acquisition enzyme activities and metabolic N limitation ($p < 0.05$), while ectomycorrhizal fungi showed the opposite pattern ($p < 0.05$). Furthermore, both the Chao1 and Shannon indices of fungal diversity were positively correlated with N-acquisition enzyme activities and metabolic N limitation.

PLS-PM was used to elucidate the potential mechanism by which stand age affected soil microbial metabolic N limitation and soil microbial community (Fig. 6). Results showed that long-term afforestation might indirectly influence the metabolic N limitation through soil N:P and C:P ($p < 0.05$). The metabolic N limitation would further directly impact the composition and alpha-diversity of fungal community ($p < 0.05$), but did not significantly influence the fungal putative function ($p > 0.05$). The proposed mechanism through which centennial afforestation influences soil metabolic N limitation and fungal community attributes was also illustrated (Fig. 6B).

4. Discussion

4.1. Progressive metabolic N limitation during afforestation

In this study, both vector analysis and the threshold model indicated a progressive increase in metabolic N limitation in soil from y10 to y160, with no corresponding limitation observed for C or P (Fig. 3). This pattern indicated that N became an increasingly constrained resource over time. The limitation could be interpreted as follows. First, soil microbial metabolism in forest ecosystem depends primarily on high C:N materials like litterfall, yet soil N accumulates more slowly than C (Kuypers et al., 2018), which makes N become a particularly valuable nutrient. Such constraint is especially pronounced in coniferous forests (e.g., Mongolian pine in this study) as their needle litter is richer in recalcitrant, high C:N compounds compared to deciduous litter (Jílková et al., 2019). Consequently, microorganisms upregulate production of N-acquisition enzymes to mobilize N from organic substrates (Bi et al., 2022). Second, competition between trees and microbes for available N further exacerbates this limitation. With increasing stand age, the rising N demand of maturing trees exacerbates N scarcity for soil microbial community. These findings aligned with previous field studies and meta-analyses that have documented widespread microbial N limitation across various afforested ecosystems (Bi et al., 2022; Liu et al., 2023; Liu et al., 2024b).

4.2. Fungal community subjected more to the microbial metabolic N limitation than bacterial community during afforestation

The tree development progressively altered microbial niches, prompting a shift in soil microbial resource acquisition strategies. The bacterial and fungal communities, however, exhibited varying responses to afforestation in terms of both alpha-diversity and community composition. The fungal community demonstrated a significant increase in alpha-diversity and substantial compositional shifts, while their variations in the bacterial community were relatively weak across the chronosequence. Both random forest model and PLS-PM results confirmed that only fungal community significantly were profoundly influenced during afforestation (Fig. 6), highlighting its functional plasticity in adapting to changing soil conditions across the chronosequence. As such, we then focused on the fungal community in the following section.

Fungi are specialized in decomposing complex organic compounds

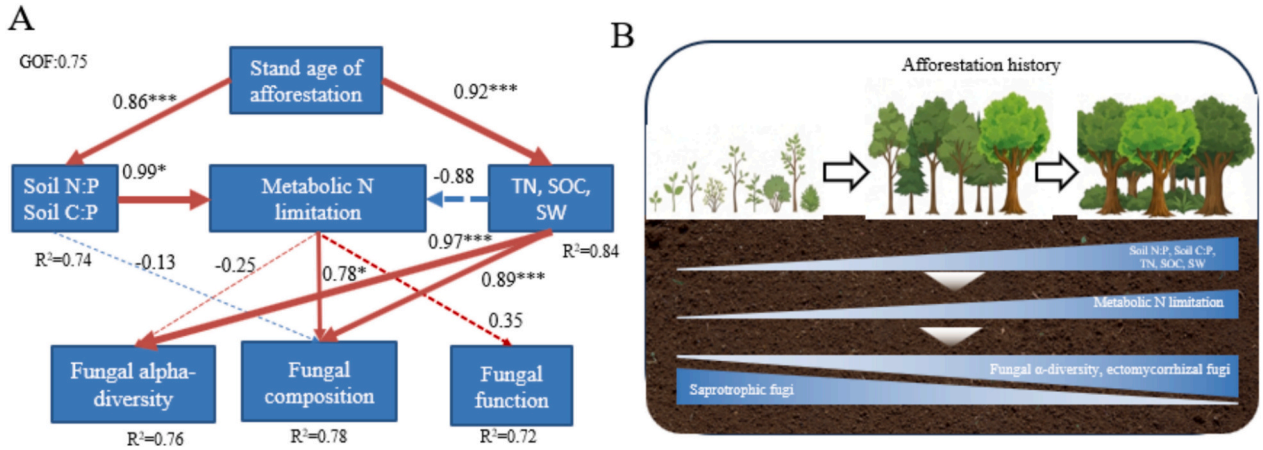

Fig. 6. Partial least squares path modeling (PLS-PM) assessing the effects of afforestation history on soil metabolic N limitation and its subsequent impacts on soil fungal community properties (A), alongside a proposed mechanism diagram (B). Fungal alpha-diversity includes Chao1 and Shannon indices. Fungal function includes ectomycorrhizal fungi, saprotroph, and root associated biotroph. The numbers next to the arrows indicate the standard path coefficients between the respective variables, with significance levels of $^{*}p < 0.05$, $^{**}p < 0.01$, and $^{***}p < 0.001$ for each predictor. The red solid and the blue solid arrows indicate positive and negative relationships, respectively. The arrow width is proportional to the strength of the coefficient. (For interpretation of the references to colour in this figure legend, the reader is referred to the web version of this article.)

like lignin polymers due to their superior C-use efficiency (Rosinger et al., 2019; Veres et al., 2015), while bacteria preferentially utilize simpler, more labile substrates (Wang and Kuzyakov, 2024). The microbial taxa enriched in this study were primarily involved in the decomposition of diverse organic matter, with fungal taxa being especially prominent. For example, Coniochaetaceae, the enriched fungal taxa in y160, are the cellulolytic and xylosis species (Duan et al., 2023). Myxotrichaceae can degrade cellulose and tannic acid, and remove cell-wall components simultaneously from plant tissues (Rice et al., 2006). *Tausonia* within Basidiomycota can produce ligninases capable of breaking down lignin-rich substrates (Wu et al., 2022). Some of the Basidiomycota degrade cellulose and insoluble phenolics, and preferentially remove the polyphenolic matrix from plant cell walls (Rice et al., 2006). Meanwhile, some enriched bacterial lineages, such as *Microlunatus* and Acidobacteriales, identified in the early afforestation stage (y10), are capable of degrading cellulose, chitin, and xylan by enhancing cellulolytic activity (Fig. S5) (Belova et al., 2018). Although we did not directly measure the chemical compositions of SOC in this study, a previous study has shown that afforestation initially promotes the accumulation of easily degradable components (evidenced by a low alkyl/O-alkyl ratio), followed by a gradual shift toward lignin-derived phenols in later stages (Song et al., 2023). This transition likely explained why more fungal lineages enriched than bacterial groups in the older stands. Due to their narrow niche width (Fig. S4), soil fungal community is more sensitive to environmental disturbances. In support, great variations of fungal community to afforestation have been reported in both subtropical and temperate forests (He et al., 2023; Huang et al., 2023).

Our analysis further revealed that soil fungal community properties, namely diversity, composition, and associated functional group, were strongly impacted by soil enzymatic properties. Regarding alpha-diversity, we found that fungal community with high richness and diversity was linked to high enzyme activities and the metabolic N limitation (Fig. 5). This pattern could be ascribed to niche overlap among fungal species. As fungal community diversity increased, competitions among those species for limited N sources intensified (Chroumpi et al., 2021), driving the elevated production of enzyme (in particular N-acquisition enzymes) to meet metabolic demands. The specific microbial taxa enriched, along with their predicted functions, support the finding of increased N-acquisition enzyme activity. For example, ectomycorrhizal fungi are widespread in temperate forests (Terrer et al., 2016). They are known for their symbiotic role in N absorption, and contributions to soil N cycling by producing extracellular enzymes that mineralize complex organic compounds (e.g., chitin, peptides) (Chari et al., 2024; Rúa et al., 2015). The significantly enriched ectomycorrhizal fungi in this study included Cortinariaceae (Cortinarius), *Russula*, and *Cladophialophora* (Liimatainen et al., 2022; Usui et al., 2016; Yu et al., 2020). Other mycorrhizal fungi, such as ericoid mycorrhizae, *Sebacinales* and *Oidiodendron* enriched in y80, could also produce C- and N-cycle related extracellular enzymes to decompose macromolecules (Ray et al., 2025). Under the nutrient limitation with low mineralization and nutrients largely bound in complex organic forms, ectomycorrhizal fungi enhance both their capacity and growth by utilizing energy from host-derived sugars to power nutrient mobilization, and supply host plants with the N needed to sustain their growth (Terrer et al., 2016). N immobilization in mycorrhizal mycelium proliferation and host growth may further intensify N limitation with a potential feedback on fungal community composition (Kyaschenko et al., 2017). This mechanism explains the positive relationship between the metabolic N limitation and the ectomycorrhizal fungi observed in this study (Fig. 5). In contrast, free-living saprotroph showed the negative correlation with N-acquisition enzymes and the metabolic N limitation (Fig. 5). Saprotrophic fungi rely on decomposing dead organic matter to obtain energy and nutrients, and also well-known for their capacity to produce extracellular enzymes, such as proteases, and chitinases, and, thus, can accelerate the mineralization of organic N (Wang et al., 2025). However, saprotrophic and mycorrhizal fungi have overlapping fundamental niches, but that antagonistic mycorrhizal fungi exclude more efficient saprotrophs in organic matter decomposition (Kyaschenko et al., 2017), particularly when the soil C:N ratio is relatively low(<19.7, as in our study) (Fernandez and See, 2025). Under N-limiting conditions, ectomycorrhizal fungi favor organic N uptake, increasing the likelihood of competitive interactions with saprotrophic fungi (Fernandez and See, 2025). As such, the enriched saprotrophic fungi primarily occurred during the early stages of afforestation (e.g., y0 and y10), such as *Hyphodontia, Sagenomella*, *Infundichalara*, Lipomycetaceae, and *Geminibasidium* (Fig. S2), when the relative abundance of mycorrhizal fungi was relatively low. Notably, due to this antagonistic relationship, metabolic N limitation did not exert a significant effect on predicted fungal functions in our analysis (Fig. 6).

5. Conclusions

Our study demonstrated the substantial impact of afforestation on microbial metabolic limitation and associated soil microbial community across a century-long history. As the forest aged, there were considerable changes in soil chemical properties, enzymatic activities, and microbial properties. The microbial metabolic N limitation exhibited a progressive exacerbation across the afforestation chronosequence. The soil fungal community, rather than the bacterial community, was profoundly influenced by the soil metabolic N limitation during the afforestation. Specifically, typical ectomycorrhizal fungi were significantly enriched and positively correlated with metabolic N limitation, while the saprotrophic fungi showed the opposite pattern.

Several limitations in this study warrant attention. First, litter properties (including quality, quantity, and decomposition rate) are critical drivers of microbial metabolism. Monitoring the litter dynamics is essential to fully elucidate the microbial mechanism in a more precise way. Second, the identified roles of ectomycorrhizal and saprotrophic fungi are primarily based on statistical approaches, lacking direct mechanistic evidence. Future work should employ isotope tracing techniques combined with multi-omics approaches (e.g., metagenomics and transcriptomics) to detect the expression of enzyme-encoding genes under varying N availability. Such efforts would provide a deeper understanding of how forest stand age regulates soil microbial metabolic limitations during afforestation.

CRediT authorship contribution statement

Jiangbing Xu: Writing – review & editing, Writing – original draft, Visualization, Validation, Supervision, Software, Methodology, Investigation, Formal analysis, Data curation. **Yuhao Wu:** Investigation, Data curation. **Song Jin:** Writing – original draft, Visualization, Validation, Software. **Haiquan Guo:** Resources, Project administration, Funding acquisition, Data curation. **Lei Liu:** Writing – original draft, Visualization, Validation, Software, Resources, Formal analysis, Data curation. **Jing Meng:** Validation, Resources, Project administration, Investigation. **Guoyi Zhou:** Writing – review & editing, Visualization, Validation, Supervision, Resources, Investigation, Conceptualization.

Declaration of competing interest

The authors declare that they have no known competing financial interests or personal relationships that could have appeared to influence the work reported in this paper.

Acknowledgements

This work was supported by the National Natural Science Foundation of China (grant number 42130506), the Special Technology Innovation Fund of C Peak and C Neutrality in Jiangsu Province (BK20231515), and the Technical Exploration of Surface Substrate Investigation—Research

on Methodology System from Geological Exploration Technology Center of Hebei Bureau of Geology and Mineral Resources Exploration (grant number 13000023P006CA410288Y).

Appendix A. Supplementary data

Supplementary data to this article can be found online at https://doi.org/10.1016/j.catena.2026.110003.

Data availability

PRJNA1208408 (Original data) (NCBI)

References

Belova, S.E., Ravin, N.V., Pankratov, T.A., Rakitin, A.L., Ivanova, A.A., Beletsky, A.V., et al., 2018. Hydrolytic capabilities as a key to environmental success: chitinolytic and cellulolytic Acidobacteria from acidic sub-arctic soils and boreal peatlands. Front. Microbiol. 9, 2775. https://doi.org/10.3389/fmicb.2018.02775.

Bi, B., Wang, Y., Wang, K., Zhang, H., Fei, H., Pan, R., Han, F., 2022. Changes in microbial metabolic C- and N- limitations in the rhizosphere and bulk soils along afforestation chronosequence in desertified ecosystems. J. Environ. Manage. 303, 114215. https://doi.org/10.1016/j.jenvman.2021.114215.

Bonan, G.B., 2008. Forests and climate change: Forcings, feedbacks, and the climate benefits of forests. Science 320, 1444–1449. https://doi.org/10.1126/science.1155121.

Chari, N.R., Muratore, T.J., Frey, S.D., Winters, C.L., Martinez, G., Taylor, B.N., 2024. Long-term soil warming drives different belowground responses in arbuscular mycorrhizal and ectomycorrhizal trees. Glob. Chang. Biol. 30, e17550. https://doi.org/10.1111/gcb.17550.

Chroumpi, T., Peng, M., Aguilar-Pontes, M.V., Müller, A., Wang, M., Yan, J., et al., 2021. Revisiting a 'simple' fungal metabolic pathway reveals redundancy, complexity and diversity. Microbial Biotechnology 14, 2525–2537. https://doi.org/10.1111/1751-7915.13790.

Criquet, S., Braud, A., 2008. Effects of organic and mineral amendments on available P and phosphatase activities in a degraded Mediterranean soil under short-term incubation experiment. Soil Tillage Res. 98, 164–174. https://doi.org/10.1016/j.still.2007.11.001.

Cui, Y., Wang, X., Zhang, X., Ju, W., Duan, C., Guo, X., et al., 2020. Soil moisture mediates microbial carbon and phosphorus metabolism during vegetation succession in a semiarid region. Soil Biol. Biochem. 147, 107814. https://doi.org/10.1016/j.soilbio.2020.107814.

Cui, Y.X., Moorhead, D.L., Guo, X.B., Peng, S.S., Wang, Y.Q., Zhang, X.C., Fang, L.C., 2021. Stoichiometric models of microbial metabolic limitation in soil systems. Glob. Ecol. Biogeogr. 30, 2297–2311. https://doi.org/10.1111/geb.13378.

Cui, Y.X., Moorhead, D.L., Peng, S.S., Sinsabaugh, R.L., 2023. New insights into the patterns of ecoenzymatic stoichiometry in soil and sediment. Soil Biol. Biochem. 177, 108910. https://doi.org/10.1016/j.soilbio.2022.108910.

Cui, Y., Moorhead, D.L., Peng, S., Sinsabaugh, R.L., Peñuelas, J., 2024. Predicting microbial nutrient limitations from a stoichiometry-based threshold framework. Innov Geosci 2, 100048. https://doi.org/10.59717/j.xinn-geo.2024.100048.

Daunoras, J., Kačergius, A., Gudiukaitė, R., 2024. Role of soil microbiota enzymes in soil health and activity changes depending on climate change and the type of soil ecosystem. Biology 13, 85. https://doi.org/10.3390/biology13020085.

Deng, L., Peng, C., Huang, C., Wang, K., Liu, Q., Liu, Y., et al., 2019. Drivers of soil microbial metabolic limitation changes along a vegetation restoration gradient on the loess plateau, China. Geoderma 353, 188–200. https://doi.org/10.1016/j.geoderma.2019.06.037.

Douglas, G.M., Maffei, V.J., Zaneveld, J.R., Yurgel, S.N., Brown, J.R., Taylor, C.M., et al., 2020. PICRUSt2 for prediction of metagenome functions. Nat. Biotechnol. 38, 685–688. https://doi.org/10.1038/s41587-020-0548-6.

Du, Y., Wei, Y., Zhou, Y., Wang, Y., Zhang, A., Wang, T., Li, Z., 2024. Temporal variation of microbial nutrient limitation in citrus plantations: insights from soil enzyme stoichiometry. Environ. Res. 258, 119275. https://doi.org/10.1016/j.envres.2024.119275.

Duan, Y., Chen, L., Li, Y., Li, J., Zhang, C., Ma, D., et al., 2023. Nitrogen input level modulates straw-derived organic carbon physical fractions accumulation by stimulating specific fungal groups during decomposition. Soil Tillage Res 225, 105560. https://doi.org/10.1016/j.still.2022.105560.

Fernandez, C.W., See, C.R., 2025. The pH influence on ectomycorrhizal nitrogen acquisition and decomposition. New Phytol. 867–875. https://doi.org/10.1111/nph.70021.

He, D., Guo, Z., Shen, W., Ren, L., Sun, D., Yao, Q., Zhu, H., 2023. Fungal communities are more sensitive to the simulated environmental changes than bacterial communities in a subtropical forest: the single and interactive effects of nitrogen addition and precipitation seasonality change. Microb. Ecol. 86, 521–535. https://doi.org/10.1007/s00248-022-02092-8.

Huang, K., Guo, Z., Zhao, W., Song, C., Wang, H., Li, J., et al., 2023. Response of fungal communities to afforestation and its indication for forest restoration. Forest Ecosystems 10, 100125. https://doi.org/10.1016/j.fecs.2023.100125.

Jiang, S., Xing, Y., Liu, G., Hu, C., Wang, X., Yan, G., Wang, Q., 2021. Changes in soil bacterial and fungal community composition and functional groups during the succession of boreal forests. Soil Biol. Biochem. 161, 108393. https://doi.org/10.1016/j.soilbio.2021.108393.

Jílková, V., Jandová, K., Sim, A., Thornton, B., Paterson, E., 2019. Soil organic matter decomposition and carbon sequestration in temperate coniferous forest soils affected by soluble and insoluble spruce needle fractions. Soil Biol. Biochem. 138, 107595. https://doi.org/10.1016/j.soilbio.2019.107595.

Kuypers, M.M.M., Marchant, H.K., Kartal, B., 2018. The microbial nitrogen-cycling network. Nat. Rev. Microbiol. 16, 263–276. https://doi.org/10.1038/nrmicro.2018.9.

Kyaschenko, J., Clemmensen, K.E., Hagenbo, A., Karltun, E., Lindahl, B.D., 2017. Shift in fungal communities and associated enzyme activities along an age gradient of managed *Pinus sylvestris* stands. ISME J. 11, 863–874. https://doi.org/10.1038/ismej.2016.184.

Liang, Y.M., Pan, F.J., Ma, J.M., Yang, Z.Q., Yan, P.D., 2021. Long-term forest restoration influences succession patterns of soil bacterial communities. Environ. Sci. Pollut. Res. 28, 20598–20607. https://doi.org/10.1007/s11356-020-11849-y.

Liimatainen, K., Kim, J.T., Pokorny, L., Kirk, P.M., Dentinger, B., Niskanen, T., 2022. Taming the beast: a revised classification of *Cortinariaceae* based on genomic data. Fungal Divers. 112, 89–170. https://doi.org/10.1007/s13225-022-00499-9.

Liu, C., Cui, Y., Li, X., Yao, M., 2021. *Microeco*: an R package for data mining in microbial community ecology. FEMS Microbiol. Ecol. 97, fiaa255. https://doi.org/10.1093/femsec/fiaa255.

Liu, G., Wang, H., Yan, G., Wang, M., Jiang, S., Wang, X., et al., 2023. Soil enzyme activities and microbial nutrient limitation during the secondary succession of boreal forests. Catena 230, 107268. https://doi.org/10.1016/j.catena.2023.107268.

Liu, L., Zhu, Q., Wen, D., Yang, L., Ni, K., Xu, X., et al., 2024a. Stimulation of organic N mineralization by N-acquiring enzyme activity alleviates soil microbial N limitation following afforestation in subtropical karst areas. Plant and Soil 504, 879–894. https://doi.org/10.1007/s11104-024-06668-w.

Liu, L., Zhu, Q., Yang, L., Elrys, A.S., Sun, J., Ni, K., et al., 2024b. Afforestation increases soil inorganic N supply capacity and lowers plant N limitation in subtropical karst areas. Geoderma 443, 116848. https://doi.org/10.1016/j.geoderma.2024.116848.

Moorhead, D.L., Sinsabaugh, R.L., Hill, B.H., Weintraub, M.N., 2016. Vector analysis of ecoenzyme activities reveal constraints on coupled C, N and P dynamics. Soil Biol. Biochem. 93, 1–7. https://doi.org/10.1016/j.soilbio.2015.10.019.

Odriozola, I., Martinovic, T., Bahnmann, B.D., Ryšánek, D., Mašínová, T., Sedlak, P., et al., 2020. Stand age affects fungal community composition in a central European temperate forest. Fungal Ecol. 48, 100985. https://doi.org/10.1016/j.funeco.2020.100985.

Ray, M., Choudhary, S., Jose, A.K., Kumar, V., Gupta, A., Bhagat, S., 2025. A complete review on ericoid mycorrhiza: an understudied fungus in the ericaceae family. Nat. Environ. Pollut. Technol. 24, B4252. https://doi.org/10.46488/NEPT.2025.v24i02.B4252.

Rice, A.V., Tsuneda, A., Currah, R.S., 2006. *In vitro* decomposition of *Sphagnum* by some microfungi resembles white rot of wood. FEMS Microbiol. Ecol. 56, 372–382. https://doi.org/10.1111/j.1574-6941.2006.00071.x.

Rosinger, C., Rousk, J., Sandén, H., 2019. Can enzymatic stoichiometry be used to determine growth-limiting nutrients for microorganisms? - a critical assessment in two subtropical soils. Soil Biol. Biochem. 128, 115–126. https://doi.org/10.1016/j.soilbio.2018.10.011.

Rúa, M.A., Moore, B., Hergott, N., Van, L., Jackson, C.R., Hoeksema, J.D., 2015. Ectomycorrhizal fungal communities and enzymatic activities vary across an ecotone between a forest and field. J. Fungi (Basel) 1, 185–210. https://doi.org/10.3390/jof1020185.

Saiya-Cork, K.R., Sinsabaugh, R.L., Zak, D.R., 2002. The effects of long term nitrogen deposition on extracellular enzyme activity in an *Acer saccharum* forest soil. Soil Biol. Biochem. 34, 1309–1315. https://doi.org/10.1016/S0038-0717(02)00074-3.

Sinsabaugh, R.L., Follstad Shah, J.J., 2012. Ecoenzymatic stoichiometry and ecological theory. Annu. Rev. Ecol. Evol. Syst. 43, 313–343. https://doi.org/10.1146/annurev-ecolsys-071112-124414.

Sinsabaugh, R.L., Lauber, C.L., Weintraub, M.N., Ahmed, B., Allison, S.D., Crenshaw, C., et al., 2008. Stoichiometry of soil enzyme activity at global scale. Ecol. Lett. 11, 1252–1264. https://doi.org/10.1111/j.1461-0248.2008.01245.x.

Song, X., Guo, J., Wang, X., Du, Z., Ren, R., Lu, S., He, C., 2023. Afforestation alters the molecular composition of soil organic matter in the central loess plateau of China. Forests 14, 1502. https://doi.org/10.3390/f14071502.

Sukhbaatar, G., Nachin, B., Purevragchaa, B., Ganbaatar, B., Mookhor, K., Tseveen, B., Gradel, A., 2019. Which selective logging intensity is most suitable for the maintenance of soil properties and the promotion of natural regeneration in highly continental scots pine forests?–results 19 years after harvest operations in Mongolia. Forests 10, 141. https://doi.org/10.3390/f10020141.

Terrer, C., Vicca, S., Hungate, B.A., Phillips, R.P., Prentice, I.C., 2016. Mycorrhizal association as a primary control of the CO_2 fertilization effect. Science 353, 72–74. https://doi.org/10.1126/science.aaf4610.

Usui, E., Takashima, Y., Narisawa, K., 2016. *Cladophialophora inabaensis* sp. nov., a new species among the dark septate endophytes from a secondary forest in Tottori. Japan. Microbes Environ 31, 357–360. https://doi.org/10.1264/jsme2.ME16016.

Veres, Z., Kotroczó, Z., Fekete, I., Tóth, J.A., Lajtha, K., Townsend, K., Tóthmérész, B., 2015. Soil extracellular enzyme activities are sensitive indicators of detrital inputs and carbon availability. Appl Soil Ecol 92, 18–23. https://doi.org/10.1016/j.apsoil.2015.03.006.

Wan, P., Peng, H., Ji, X., Chen, X., Zhou, H., 2021. Effect of stand age on soil microbial communities of a plantation *Ormosia hosiei* forest in southern China. Ecol Inform 62, 101282. https://doi.org/10.1016/j.ecoinf.2021.101282.

Wang, C., Kuzyakov, Y., 2024. Mechanisms and implications of bacterial-fungal competition for soil resources. ISME J. 18, wrae073. https://doi.org/10.1093/ismejo/wrae073.

Wang, A.N., Zhang, Y.F., Wang, G.L., Zhang, Z.Q., 2024. Soil physicochemical properties and microorganisms jointly regulate the variations of soil carbon and nitrogen cycles along vegetation restoration on the loess plateau, China. Plant and Soil 494, 413–436. https://doi.org/10.1007/s11104-023-06290-2.

Wang, J.Y., Li, Y.Y., Ji, Y.B., He, J., Zhang, J.H., Dong, Z.H., et al., 2025. Biodiversity of key soil phylotypes is associated with increased plant richness and productivity following agricultural abandonment and afforestation. J. Ecol. 113, 403–417. https://doi.org/10.1111/1365-2745.14463.

Wu, J., Shi, Z., Zhu, J., Cao, A., Fang, W., Yan, D., et al., 2022. Taxonomic response of bacterial and fungal populations to biofertilizers applied to soil or substrate in greenhouse-grown cucumber. Sci. Rep. 12, 18522. https://doi.org/10.1038/s41598-022-22673-4.

Yadav, A.N., Kour, D., Kaur, T., Devi, R., Yadav, A., Dikilitas, M., et al., 2021. Biodiversity, and biotechnological contribution of beneficial soil microbiomes for nutrient cycling, plant growth improvement and nutrient uptake. Biocatalysis and Agricultural Biotechnology 33, 102009. https://doi.org/10.1016/j.bcab.2021.102009.

Yan, B., Duan, M., Wang, R., Li, J., Wei, F., Chen, J., et al., 2022. Planted forests intensified soil microbial metabolic nitrogen and phosphorus limitation on the Loess Plateau, China. Catena 211, 105982. https://doi.org/10.1016/j.catena.2021.105982.

Yao, X., Zeng, W., Zeng, H., Wang, W., 2020. Soil microbial attributes along a chronosequence of scots pine (*Pinus sylvestris* var. *mongolica*) plantations in northern China. Pedosphere 30, 433–442. https://doi.org/10.1016/S1002-0160(17)60329-1.

Yu, F., Liang, J.F., Song, J., Wang, S.K., Lu, J.K., 2020. Bacterial community selection of *Russula griseocarnosa* mycosphere soil. Front. Microbiol. 11, 347. https://doi.org/10.3389/fmicb.2020.00347.

Zhao, M., Chen, Y., Zhang, Y., 2025. Effects of stand density on soil enzyme activities and microbial metabolic limitation in differently aged *Robinia pseudoacacia* Linnaeus plantations. Appl. Soil Ecol. 215, 106441. https://doi.org/10.1016/j.apsoil.2025.106441.

Zheng, Y., Ye, J., Pei, J., Fang, C., Li, D., Ke, W., et al., 2024. Initial soil condition, stand age, and aridity alter the pathways for modifying the soil carbon under afforestation. Sci. Total Environ. 946, 174448. https://doi.org/10.1016/j.scitotenv.2024.174448.